Molybdenum carbides, active and *in situ* regenerable catalysts in hydroprocessing of fast pyrolysis bio-oil

Jae-Soon Choi,[a,*] Alan H. Zacher,[b] Huamin Wang,[b] Mariefel V. Olarte,[b] Beth L. Armstrong,[a] Harry M. Meyer III,[a] I. Ilgaz Soykal,[a] and Viviane Schwartz[a]

[a] Oak Ridge National Laboratory, Oak Ridge, TN 37831, USA

[b] Pacific Northwest National Laboratory, Richland, WA 99352, USA

Manuscript for submission to:

Energy & Fuels

[*]Corresponding author: Jae-Soon Choi

E-mail address: choijs@ornl.gov

Tel: +1-865-946-1368; Fax: +1-865-946-1354

Notice: This manuscript has been authored by UT-Battelle, LLC under Contract No. DE-AC05-00OR22725 with the U.S. Department of Energy. The United States Government retains and the publisher, by accepting the article for publication, acknowledges that the United States Government retains a non-exclusive, paid-up, irrevocable, world-wide license to publish or reproduce the published form of this manuscript, or allow others to do so, for United States Government purposes. The Department of Energy will provide public access to these results of federally sponsored research in accordance with the DOE Public Access Plan (http://energy.gov/downloads/doe-public-access-plan).

Abstract

This paper describes properties of molybdenum carbides as a potential catalyst for fast pyrolysis bio-oil hydroprocessing. Currently, high catalyst cost, short catalyst lifetime, and lack of effective regeneration methods are hampering the development of this otherwise attractive renewable hydrocarbon technology. A series of metal-doped bulk Mo carbides were synthesized, characterized and evaluated in sequential low-temperature stabilization and high-temperature deoxygenation of a pine-derived bio-oil. During a typical 60 h run, Mo carbides were capable of upgrading raw bio-oil to a level suitable for direct insertion into the current hydrocarbon infrastructure with residual oxygen content and total acid number of upgraded oils below 2 wt% and 0.01 mg KOH g^{-1}, respectively. The performance was shown to be sensitive to the type of metal dopant, Ni-doped Mo carbides outperforming Co-, Cu-, or Ca-doped counterparts; a higher Ni loading led to a superior catalytic performance. No bulk oxidation or other significant structural changes were observed. Besides the structural robustness, another attractive property of Mo carbides was *in situ* regenerability. The effectiveness of regeneration was demonstrated by successfully carrying out four consecutive 60 h runs with a reductive decoking between two adjacent runs. These results strongly suggest that Mo carbides are a good catalyst candidate which could lead to a significant cost reduction in hydroprocessing bio-oils. We highlight areas for future research which will be needed to further understand carbide structure-function relationships and help design practical bio-oil upgrading catalysts based on Mo carbides.

Keywords: Fast pyrolysis; Bio-oil; Hydroprocessing; Hydrotreating; Deoxygenation; Molybdenum carbides; Mo_2C; Catalysts; Regeneration.

Introduction

Fast pyrolysis is a cost-effective way to produce a liquid hydrocarbon intermediate from lignocellulosic biomass.[1] The pyrolysis liquid product (aka bio-oil) is, however, not suitable for direct use as a transportation fuel or as a crude oil substitute due to undesirable qualities directly related to its high oxygen, acid and water content.[1-3] Bio-oil qualities can be improved by hydroprocessing to eliminate oxygenated functionalities.[4,5] Compared to acid-catalyzed cracking which is another major upgrading method under development, hydroprocessing has an advantage of leading to higher liquid yields and less gaseous and solid (coke and char) products.[6] Nonetheless, catalyst coking due to highly reactive bio-oil compounds is a serious challenge for hydroprocessing as well. To mitigate the rapid catalyst coking and deactivation, the current state of the art (still at various R&D stages) generally employs multiple sequential catalytic steps. A common practice is to stabilize bio-oils by hydrogenating highly reactive compounds such as carbonyls at low temperatures over a Ru/C type catalyst followed by high temperature deep deoxygenation and hydrocracking over a sulfided $CoMo/Al_2O_3$ type catalyst.[7] Despite the significant progress made in adapting catalysts developed for petroleum industry, high catalyst cost because of the using of noble metals, limited catalyst stability, and lack of effective regeneration strategies remain critical technical barriers to the development of bio-oil hydroprocessing technology.[4,5,7,8] While coking is the major deactivation mechanism responsible for fast performance loss, the existing catalysts are not amenable to *in situ* regeneration.[9,10] Furthermore, sulfided $CoMo/Al_2O_3$ type catalysts are prone to structural changes due to high water (Al_2O_3 => boehmite) and low sulfur (sulfides => oxides) contents of bio-oils.[7,8] It is therefore highly desirable to develop catalysts specifically tailored to bio-oils with excellent durability and regenerability. From a process economics perspective, it would be preferable to design catalysts which do not require precious metals and/or sulfiding agent addition during reactor operation.

Molybdenum carbides have shown to be active in various hydrocarbon conversion reactions typically catalyzed by precious metals or sulfides.[11-13] In addition, recent studies demonstrated that carbides can convert a range of oxygenated compounds found in biomass-derived feedstocks such as ethylene glycol,[14] furfural,[14,15] anisole,[16] phenol,[17] guaiacol,[18] acetic acid,[19] and levulinic acid.[20] Some reports indicate that Mo carbides can transform these compounds even in the presence of a water,[17-19] which is a positive catalyst property considering

high water concentrations found in many biomass conversion processes. However, there are also concerns about the long-term structural robustness of Mo carbides particularly with respect to bulk oxidation by water due to their high oxygen affinity.[17,19] While a significant amount of information is available in the literature on the performance of RuS_x/C and NiMoS/A_2O_3 type catalysts, little is known about the performance of Mo carbides in real bio-oil hydroprocessing which involves a range of oxygenated hydrocarbons and high concentration water.

In the present work, we have attempted to answer this question of how active and stable Mo carbides are in real hydroprocessing conditions compared with more conventional catalysts. To the best of our knowledge, this is the first paper reporting on the performance of Mo carbides in 2-stage hydroprocessing of raw bio-oil. This paper describes promising activity, stability, and *in situ* regenerability of Mo carbides and suggests areas for future research and fundamental understanding needed to develop a novel class of bio-oil hydroprocessing catalysts based on Mo carbides.

Experimental

Catalysts

All carbide catalysts were prepared by a classical temperature-programmed carburization (TPC) method.[21] As precursors for carbide synthesis, Ca-, Co-, Ni, or Cu-doped MoO_3 beads were prepared using a gelation method.[22] First, a batch of slurry was prepared by suspending MoO_3 powder (Alfa Aesar) in an aqueous solution of sodium alginate. When the oxide slurry bead was dropped into an aqueous solution of a metal chloride ($CaCl_2$, $CoCl_2$, $NiCl_2$, or $CuCl_2$), Na^+ ions in the alginate binder exchange with the divalent metal ions (e.g., one Ca^{2+} ion for two Na^+ ions) giving rise to cross-linkage among alginate polymer molecules. The cross-linking led to the formation of rigid MoO_3 beads. The concentration of metal chloride solution was 2 wt%. In the case of $NiCl_2$, a higher concentration (6 wt%) was also used to increase the Ni doping level of MoO_3 beads. The precipitated oxide beads were separated from the aqueous solution, rinsed, dried, and heat-treated at 600 °C for 2 h in air to remove binder-derived hydrocarbons and produce doped MoO_3 beads. Carburization of metal-doped MoO_3 beads was carried out via the TPC method. In a carburizing gas consisting of 15% CH_4 and 85% H_2 (flow rate: 104 sccm per gram of precursor), the sample temperature was raised from room temperature to 700 °C at 1 °C/min and soaked at the final temperature for 1 h. After cooling down to room temperature,

the synthesized carbides were passivated in a 1% O_2/N_2 flow for 12 h. Five Mo carbide samples were prepared for this study and represented by Ni-Mo_2C (Ni doping), Ni-Mo_2C-H (higher Ni-doping), Cu-Mo_2C (Cu-doping), Co-Mo_2C (Co-doping), and Ca-Mo_2C (Ca-doping).

As a baseline catalyst system representing the state of the art, sulfided Ru/C and sulfided $NiMo/Al_2O_3$ catalysts were used to conduct the baseline test. The Ru/C with a Ru loading of 7.8 wt% was prepared in house and the $NiMo/Al_2O_3$ was a commercial product.

Characterization

X-ray diffraction patterns were recorded on a powder X-ray diffractometer (X'Pert PRO, PANalytical, Almelo, Netherlands) operated at 45 kV and 40 mA using CuKα radiation (Kα = 0.154178 nm). Solid phase identification was done using the International Centre for Diffraction Data (ICDD) library: Mo_2C (04-004-8327), Mo (00-001-1205), MoO_2 (00-002-0422), and Fe_3O_4 (00-001-1111). The crystallite sizes (D_c) were estimated from the Scherrer equation using commercial software (HighScore Plus). The full width at half maximum (FWHM) and position of the peaks were calculated by profile fitting. Before the fitting, background and Kα2 of XRD peaks were removed and the peak broadening effect was adjusted using LaB_6 as a standard sample. FWHM values of (101) plane and a shape factor of 0.94 were used.

The specific surface area and porosity of catalyst samples were determined by measuring N_2 adsorption isotherms using an automatic volumetric adsorption apparatus (Quantachrome, Autosorb-1-C). Surface areas were calculated using the Brunauer-Emmett-Teller (BET) equation and the pore volumes and average pore sizes were determined using the Barrett-Joyner-Halenda (BJH) method. Average particle sizes were estimated from the equation $D_p = f/(\rho Sg)$,[23] where f is a shape factor and ρ is the density of Mo_2C (9.098 g/cc). A shape factor of 6 was applied assuming spherical particles.

The bulk content of Mo, Na, Ca, Co, Ni, and Cu in the fresh carbide catalysts as well as that of mineral species deposited during hydroprocessing testing were determined by inductively coupled plasma atomic emission spectroscopy (ICP-AES), while that of C was measured by a combustion method. Surface chemical composition and oxidation state of Mo were analyzed by X-ray photoelectron spectroscopy using a Thermo Scientific K-Alpha XPS instrument. The K-Alpha uses Al-Kα X-rays focused to a spot 400 microns in diameter. Emitted photoelectrons were energy analyzed using a 180° double focusing hemispherical analyzer with a 128-channel

detector. Survey data were collected at a pass energy of 200 eV and an energy resolution of 1 eV/step, while core level data were collected at 50 eV pass energy and 0.1 eV/step energy resolution. Sample charging was eliminated by using the K-Alpha's dual-beam charge compensation source which uses both low energy Ar-ion and low energy electrons. An Ar-ion gun (operated at 2 kv) was used for *in situ* cleaning of the sample surface. Data were collected and analyzed using the Avantage data system (v.4.61).

Temperature programmed reduction (TPR) experiments were carried out using Micromeritics AutoChem II 2920 instrument equipped with a mass spectrometer (MS) for continuous monitoring of the effluent gas composition. Sample size was less than 10 mg to prevent MS signal saturation. After flushing the sample holder with flowing 10% H_2/Argon, the temperature was increased at a rate of 10 °C/min from room temperature to 600 °C followed by a 1 h soak at 600 °C. The mass fragments detected ranged from m/z = 2 to m/z = 44; 16 and 18 for H_2O, 15 and 16 for CH_4, and 44 for CO_2.

2-stage hydroprocessing of fast pyrolysis bio-oil

The catalysts were tested for the 2-stage hydroprocessing of fast pyrolysis bio-oil at Pacific Northwest National Laboratory (PNNL). A batch of pyrolysis oil produced by the Technical Research Center of Finland (VTT) from softwood forest residues was used. Detailed analysis of the bio-oil will be reported in the later section. The hydroprocessing tests were conducted in a bench-scale hydrotreater (see Fig. 1), which was configured as a single pass, cocurrent, continuous, down-flow reactor. The system can operate at up to 12.4 MPa (1800 psig) with a maximum catalyst temperature of 400 °C. The reactor has been described in detail elsewhere by Elliott et al.[24] Catalysts were loaded in two stages heated at different temperatures to form a two-stage catalyst bed for the hydroprocessing runs. Detailed catalyst bed configurations and temperature profiles employed for individual tests were shown in Fig. S1 of Supporting Information. Each test was conducted over 60 h on stream, and the products and data were collected over the entire period with individual products and data sets collected every 6 h. The hydrogen consumption has been calculated and the yield of gas and oil products determined.

For the tests using carbide catalysts, the catalyst beds were reduced *in situ* in flowing H_2 (3-5 sccm H_2/cc catalyst) at 12.6 MPa with heating from room temperature to 250 °C at 120 °C/h and holding for 2 h before hydrotreating test. For the baseline test using sulfide catalysts, the

catalyst bed was sulfided *in situ* at 12.4 MPa by the following procedure: heating to 150 °C at 120 °C/h in H_2 flow, heating from 150 to 400 °C at 83 °C/h in a flow of H_2 and sulfiding agent consisting of 35% di-tert-butyl-disulfide (DTBDS) in decane, and then holding at 400 °C for 4 h with H_2 and sulfiding agent flowing. After each test, the catalyst beds were rinsed with acetone and spent catalysts were collected for analysis. For the catalyst regeneration tests, the catalyst beds were rinsed with acetone after a 60 h run, dried at room temperature in flowing N_2, and then treated in flowing H_2 (0.7 sccm H_2/cc catalyst) at 12.6 MPa by the following procedure: heating to 250 °C at 120 °C/h, holding at 250 °C for 2 h, heating to 425 °C at 117 °C/h, and then holding at 425 °C for 4 h.

The bio-oil feed and the hydrotreated products were analyzed at PNNL for elemental analysis (ASTM D5291 for C, H, N; ASTM D5373 for O; and ASTM D1552 for S), total acid number (TAN, ASTM D3339), water content (ASTM D6869), and density (Stabinger apparatus, ASTM D7042). In addition, the products were analyzed by simulated distillation (ASTM D2887).

Results and discussion

Physicochemical properties of fresh Mo carbide catalysts

Consistent with the literature data,[19,21] the temperature programmed carburization of Mo oxide precursors led to carbides with hexagonal close packed (hcp) Mo_2C structures except for Ca-doped MoO_3 (Fig. 2). No crystalline phases related to Na (alginate binder residues) or dopants (Ca, Co, Ni, Cu) were observed likely due to their low contents (Table 1). It has been reported that even small amounts of metal dopants can affect MoO_3 carburization and resulting carbide structures. Kojima and Aika, for example, showed that Cs addition inhibits carburization with Mo metal as the major product.[25] The presence of two alkali-character metals (i.e., Na and Ca) in the Ca-doped MoO_3 could therefore explain the incomplete carburization resulting in a mixture consisting of Mo_2C, Mo and MoO_2. Although the other precursors also had Na residues, it did not prevent the formation of pure Mo_2C phases (Fig. 2). The apparent inconsistency is likely due to the compensating effect of Co, Ni, and Cu dopants. Jung et al. in fact found that these metals can facilitate oxide reduction during MoO_3 carburization.[26] Furthermore, the authors observed that Ni doping favors fcc α-MoC_{1-x} while Co and Cu lead to hcp Mo_2C formation. The fact that all of the Co, Ni, and Cu-doped MoO_3 precursors were carburized to hcp Mo_2C in the present work, further supports the idea of combined influence of Na residue and metal dopants.

As summarized in Table 2, the prepared carbides had surface areas ranging from 9 to 23 m^2/g which are moderate but considerably higher than the initial MoO_3 surface area of less than 1 m^2/g. Ca-Mo_2C had a lower 2 m^2/g due to the delayed and incomplete carburization as described above. All the catalysts possessed low porosity (0.03-0.06 cc/g) with pore sizes in the mesopore range. As we observed in a previous work where Mo_2C was synthesized from undoped Mo oxides using the same carburization procedure employed in the present study, the particle sizes estimated from the BET surface areas were significantly higher than the crystallite sizes determined by XRD.[19] The difference between particle and crystallite sizes implies that several crystallites were tightly combined as a particle and/or non-carbidic carbon deposits blocked access to inter-crystallite spaces.[19,21] Given that bulk C/Mo ratios were higher than 0.5 (stoichiometric value for pure Mo_2C) and C concentrations were higher on the surface than in the bulk (see Tables 1 and 3), it is reasonable to conclude that non-carbidic carbon species (e.g., polymeric or graphitic) formed during carburization led to some degree of pore blocking and masking of active sites. As non-carbidic carbon species deposited during carburization can be removed by reductive treatments,[21] some of the pore-blocking C species could have been removed under the high H_2 pressures used in the present study. Additional characterization (e.g., XPS after a treatment under H_2 pressure) will be needed to understand the stability of non-carbidic carbon species in hydroprocessing conditions and impact on performance.

Besides these non-carbidic carbon species denoted by C (C-C) in Table 4, carbon species associated with oxygen denoted by C (C-O) were also present (for representative XPS spectra and peak fit results, see Fig. S2 in Supporting Information). The latter were likely carbonates formed during passivation along with Mo oxides which prevented bulk oxidation of Mo_2C (a pyrophoric material) upon exposure to ambient air. Generally, passivation layers can be removed by a reductive treatment done before activity measurements, even though some oxygen residues can persist.[27] In regard to dopant distribution, Ca concentration was higher on the surface of Ca-Mo_2C than in the bulk (compare Tables 1 and 3). By contrast, Co, Ni, and Cu dopants were rather uniformly distributed. Overall, the bulk concentrations of metal dopants were close to one another at 0.2-0.3% except for Ni-Mo_2C-H which had ca. 0.8% Ni. As described in the experimental section, the oxide precursor for the latter sample was prepared using a 6 wt% metal chloride solution instead of 2 wt% in an effort to increase the doping level.

Bio-oil hydroprocessing performance

To understand Mo carbides' ability to upgrade raw bio-oil via low-temperature stabilization and high-temperature deep hydroprocessing, each catalyst was loaded in two different temperature zones (Stages 1 and 2) of the hydrotreater. For the baseline, RuS_x/C and NiMoS/Al_2O_3 catalysts were placed in low (Stage 1) and high temperature (Stage 2) zones, respectively. Table 5 summarizes catalyst loadings, mid-bed temperatures, and other relevant reaction parameters, while Fig. S1 (see Supporting Information) presents catalyst bed configurations and temperature profiles. We tried to evaluate carbides at conditions as close to those used for the baseline catalysts as possible. Nevertheless, there were some discrepancies due to intrinsically different bulk densities between supported (RuS_x/C, NiMoS/Al_2O_3) and bulk (Mo_2C) catalysts. For instance, while space velocities on a catalyst volume basis (LHSV) were higher for Mo carbides, those on a catalyst weight basis were higher for the baseline catalysts. In addition, for most of the carbide evaluations a portion of the temperature transition zone (Stage 1 => Stage 2) was filled with quartz beads instead of catalysts (Fig. S1). Despite these differences, however, we believe that our comparison among different carbides and baseline catalysts can give us meaningful information about the potential of carbides in real bio-oil hydroprocessing.

With respect to overall product yields, the Mo carbides except Ca-Mo_2C led to oil, gas and aqueous-phase yields comparable to those obtained over the baseline catalysts (Fig. 3). In the case of Ca-Mo_2C, oil yield was considerably higher while aqueous phase was lower. A remarkably lower H_2 consumption (Fig. 3d) and a larger CO_2 production (Fig. 4) over Ca-Mo_2C indicate that dominant conversion pathways for this catalyst were different. The Ca-Mo_2C catalyst was also less effective in upgrading the raw bio-oil, as indicated by the higher density of the upgraded oil (Fig. 5). The density of upgraded oils can generally be correlated with its oxygen content.[28] As an example, a lower density indicates a less residual O in the oil, which in turn suggests a better deoxygenation (upgrading) activity of catalysts. The reactor experiment for Ca-Mo_2C had to be terminated after 54 h on stream due to the Stage 2 bed plugging with char and coke resulting in >100 psi pressure buildup across the catalyst bed. This clearly demonstrates that the Ca-Mo_2C catalyst was not able to sufficiently stabilize the raw bio-oil in Stage 1 letting thermally unstable compounds enter the high temperature Stage 2 bed. Polymerization of reactive bio-oil compounds competing with hydrotreating reactions is well documented in the literature.[4,5,7,29] All the other catalysts were able to operate effectively for the planned 60-h run

without bed plugging. These results thus underscore the importance of synthesizing Mo carbides without metallic Mo or MoO_2 phases to achieve good hydroprocessing activity (see carbide XRD patterns in Fig.2).

On the other hand, there were also differences between the active Mo_2C-phase only catalysts (i.e., Ni-Mo_2C, Cu-Mo_2C, Co-Mo_2C, and Ni-Mo_2C-H), and the baseline (i.e., RuS_x/C + $NiMoS/Al_2O_3$). For example, the Mo carbides had slightly lower gas yields, but higher oil yields and H_2 consumption. More notable differences were in the gas-phase composition. Indeed, significantly higher CO and CO_2 were produced over the baseline catalyst (Fig. 4) suggesting that decarbonylation and decarboxylation pathways (i.e., via C-C bond cleavage) to deoxygenation of bio-oils were less favored over Mo carbides. The relatively low CO and CO_2 production over Mo carbides seems consistent with previous model compound studies which showed that Mo carbides are selective towards cleaving C-O bonds.[15,30] Among the active carbide catalysts, Ni-Mo_2C-H was the most active achieving an upgraded oil density comparable to the baseline under the conditions optimized for the latter (Fig. 5). To obtain further insights into the upgrading performance of different catalysts, select upgraded oil samples were analyzed and results are summarized in Table 6. In agreement with the H_2 consumption (Fig. 3d) and oil density (Fig. 5) trends, significant improvements in oil properties occurred including increased H/C ratios, and reduced O, moisture and total acid numbers. As expected, remaining O and acid contents were considerable for Ca-Mo_2C. Among the carbides, Ni-Mo_2C-H produced the best quality oil with a residual O content of <2 wt% and a TAN of <0.01. These O and TAN values are comparable to those obtained over the baseline catalysts (Table 6) and can be considered suitable for integration into the current hydrocarbon infrastructure.[31] Note that the upgraded oil H/C ratios for Ni-Mo_2C-H and the baseline catalysts were similar (Table 6) while more H_2 was consumed by Ni-Mo_2C (Fig. 3d). This trend could be explained in part by the greater CO and CO_2 formation over the baseline catalyst (Fig. 4a and 4b).

According to the simulated distillation analysis, Mo carbides and the baseline catalysts generated hydrocarbon products in similar boiling point ranges (Fig. 6) with more than 70 wt% of the upgraded oils in the gasoline and diesel fractions. Among the carbides, Co-Mo_2C and Ni-Mo_2C-H stood out: the former had a considerably greater contribution from products heavier than diesel fractions, while the latter had larger gasoline and diesel fractions. This is in line with the upgrading performance trend summarized in Table 6 (see H/C, O, TAN, density values).

Based on the density of hydroprocessed oils (in g/mL) reported in Table 6, the catalytic activity of carbide catalysts can be estimated to be in the following order: Ni-Mo_2C-H (0.824) > Ni-Mo_2C (0.869) > Cu-Mo_2C (0.876) > Co-Mo_2C (0.893) > Ca-Mo_2C (0.949). As described above, the relatively poor performance of Ca-Mo_2C can be explained by the presence of Mo and MoO_2 phases. Among the other carbides, however, reasons for the activity differences are not clear at this time. Comparing the catalyst morphology data in Table 2 against the performance data in Table 6, we observe that catalyst activity does not directly correlate with surface area. In fact, although Cu-Mo_2C had a higher surface area than the other carbides, it was less active than Ni-Mo_2C and Ni-Mo_2C-H. Stellwagen and Bitter recently observed on carbon nanofiber supported Mo carbides that the activity in hydrodeoxygenation of stearic acid increased with carbide particle size.[32] This structure sensitivity was explained by difference in oxygen affinity: larger Mo_2C particle is less prone to surface oxidation, and therefore its hydrogenation function is less affected by oxygen.[32] Our results are not entirely consistent with this trend either since Co-Mo_2C despite its larger particle size was less active than Cu-Mo_2C. The apparent discrepancy suggests that even though similar particle size effects could have been applied to our bulk carbides, the intrinsic activity (i.e., activity normalized to surface area) of carbides was strongly influenced by dopant type. The amount of dopant loading seems to have played a role as well, given that a higher Ni-loading sample outperformed a lower loading counterpart (i.e., Ni-Mo_2C-H > Ni-Mo_2C). The reactivity of Mo carbides is known to be sensitive to surface composition, clean Mo_2C surfaces (i.e., minimized Mo metal, Mo oxides, and non-carbidic C) being most effective in reactions involving H_2.[26,33,34] The XPS data in Table 4 indicates that Ni-doping could have indeed favored "cleaner" carbide surfaces (*cf.* Mo (Mo-C), Mo (Mo-O) and C (C-C) contributions to the overall surface composition) thereby imparting a better hydroprocessing activity to Mo carbides. Further research will, however, be necessary to draw firm conclusions regarding the role of dopants. For instance, we cannot rule out some direct involvement of Ni in the reaction pathways. Investigating types and numbers of different active sites using probe molecules such as H_2, CO, and O_2, and comparing intrinsic activity (e.g., turnover frequency) of different carbide catalysts in model compound conversion (e.g., furfural, carboxylic acids, and guaiacol) would be especially useful.

Stability and *in situ* regenerability

As aforementioned, the evaluated catalysts except Ca-Mo_2C were able to operate for planned 60 h without noticeable bed fouling or plugging. On the other hand, more gradual activity loss was observed with time on stream for all catalysts as can be inferred from the increasing oil densities in Fig. 5. This kind of deactivation is generally attributed to catalyst surface coking which is a major technical challenge for bio-oil hydroprocessing catalysts including state-of-the-art catalysts such as our baseline.[4,5,7,9] While it is imperative to develop catalysts less prone to coking and/or process operating strategies which mitigate coke deposition, it is also highly desirable to develop catalysts that are *in situ* regenerable. In fact, given that oxygenated compounds in bio-oils are generally more susceptible to polymerization and coking than hydrocarbons in petroleum feedstock, more frequent catalyst maintenance is expected for bio-oil hydroprocessing compared to typical petroleum hydroprocessing practices. A recent techno-economic analysis by Jones et al. indeed pointed out that catalyst replacement rate has a very large effect on the overall process economics.[35] Therefore the ability to regenerate effectively in the hydroprocessing reactor could greatly reduce the conversion cost.

Two of the reactor evaluated catalysts (Ni-Mo_2C and Cu-Mo_2C) were analyzed via temperature-programmed reduction and results are summarized in Fig. 7. During a TPR experiment done from room temperature to 600 °C at atmospheric pressure, CH_4 (m/z 15) evolution was negligible from the fresh catalysts indicating that removal of carbidic C was minimal (i.e., stable carbide structure). At atmospheric pressure H_2, non-carbidic C species deposited during carburization are generally removed at higher temperatures around 700 °C,[22,34] so their contribution to CH_4 was absent from Fig. 7. The TPR profiles of the tested catalysts confirm that coke deposition occurred during 60 h hydroprocessing. For both catalysts, carbon accumulation in Stage 1 was higher, which is reasonable considering that most reactive bio-oil compounds must have been converted during stabilization in Stage 1. In contrast to Ni-Mo_2C, carbon deposition in Stage 2 was substantial on Cu-Mo_2C which seems to be in line with the activity trend discussed above (less active Cu-Mo_2C based on Table 6 oil density data). Important information which can be drawn from Fig. 7 is that deposited carbon species were quite reactive and removable at or below 600 °C. This means that regeneration of coked carbides can likely be accomplished inside the hydroprocessing reactor. In fact, under much higher pressure H_2 available in a hydroprocessing reactor, decoking would be possible at temperatures much lower than 600 °C. This is potentially a big advantage of carbide catalysts over

conventional hydroprocessing catalysts whose regeneration is typically done *ex situ* via successive oxidative coke burn off and reactivation (e.g., sulfidation).[10]

To assess the feasibility of *in situ* regeneration, the Ni-Mo_2C-H catalyst was subjected to 4 consecutive 60 h hydroprocessing runs. After an initial 60 h run, the catalyst was reduced at 425 °C for 4 h. As shown in Fig. 8, the catalyst recovered its activity (except for the initial 12 h or so break-in period) and was able to operate effectively for a second 60 h run. Even though the upgrading performance was still high (oil O content=1.55 wt%, TAN=<0.01, density=0.834 g/mL in Table 6), the reductive treatment was repeated and a third 60 h operation followed. Again, the upgraded oil quality was sufficient, but another round of regeneration was carried out. After having verified activity recovery, space velocity was doubled (WHSV: 0.288 => 0.433) to further challenge the catalyst during the 4^{th} 60 h evaluation. As apparent from Fig. 8 and Table 6, the carbide catalyst performed effectively. In summary, one batch of Mo carbide catalyst upgraded raw bio-oil successfully for 240 h generating good quality oil products and without fouling or plugging the catalyst bed.

Carbide catalysts are known for oxygen affinity. Recent studies suggest that it is the oxophilicity of Mo carbides that makes them a good catalyst in conversion of oxygenated compounds (e.g., high selectivity towards C-O bond cleavage).[36] On the other hand, that very property could make carbides more vulnerable to bulk oxidation either by H_2O or oxygenated hydrocarbons. Mortensen et al. recently reported that H_2O (either produced during deoxygenation or present as a solvent) induced gradual transformation of Mo_2C phases supported on ZrO_2 into MoO_2 phases, which in turn led to drastic activity loss in hydrodeoxygenation of phenol in 1-octanol.[17] MoO_2 formation was observed over Mo_2C/C[32] and bulk Mo_2C[19] as well during hydroprocessing of other model compounds. The bio-oil used in the present study contained about 30% water and its upgraded products had 50-60 wt% of aqueous phase. Despite operating for 240 h in this environment, the tested Ni-Mo_2C-H showed no sign of MoO_2 formation according to XRD analysis (Fig. 9). In fact, little changes could be seen between the fresh and tested states overall (e.g., similar crystallite sizes indicating the absence of sintering) demonstrating the structural robustness of Mo carbide catalysts under real bio-oil hydroprocessing conditions. Minor accumulation of Fe_2O_3 phases was detected in the tested Stage 2 bed. Unrefined raw bio-oils can contain a variety of inorganic contaminants derived from biomass, pyrolysis reactors, and/or hydroprocessing reactors[1,4,5] which can accumulate in the

hydroprocessing catalyst beds. Indeed, the ICE-AES screening done after the 240-h testing revealed the presence of other inorganic deposits on Ni-Mo_2C-H such as Ca, Cr, Mg, P, and S (Table 7). The fact that this carbide catalyst was still active at the end of the 240 h testing suggests that the activity of carbides is not very sensitive to these elements. Relative sulfur tolerance of Mo carbides compared to platinum, for instance, has previously been reported in the context of tetralin hydrogenation.[37] In practice, the inorganic content of raw bio-oils is likely to be reduced prior to the hydroprocessing steps further minimizing the possible impact of deposits. Elliott et al. reported that hot vapor filtration during fast pyrolysis oil production significantly reduced mineral content of bio-oil, although the effect of reduced mineral content on RuS_x/C and CoMoS/Al_2O_3 hydroprocessing catalyst activity was minor over a 5-day evaluation runs.[24] On the other hand, the level of Ni doping appears to have been maintained, while that of Na residue (left over from the MoO_3 precursor synthesis) decreased substantially (Table 7). In summary, Mo carbides were structurally stable and catalytically active during a 240 h evaluation. However, longer term effects of Fe_2O_3 and other inorganic deposits on upgrading performance need to be addressed in future research as well as possible evolution in surface composition for example C/O/Mo/dopant ratios.

Conclusions

This study confirms the potential of molybdenum carbides as effective catalysts for hydroprocessing of real fast pyrolysis bio-oils and suggests directions for future research needed to help develop active, stable, and *in situ* regenerable catalysts based on carbides. Main findings were:

- Molybdenum carbides were able to upgrade raw bio-oils to the level suitable for direct insertion into the current hydrocarbon infrastructure comparing favorably with the current state of the art RuS_2/C and NiMoS/Al_2O_3 catalysts in low-temperature stabilization and high-temperature deoxygenation and hydrocracking, respectively;
- Performance of molybdenum carbides was sensitive to the type of metal dopant with Ni-doped carbides generally outperforming Co-, Cu-, or Ca-doped ones;
- Carbide structures were robust under bio-oil hydroprocessing conditions; no bulk oxidation or major structural changes were observed during 240 h operation;

- Carbon species deposited during bio-oil hydroprocessing were reactive and removable by a hydrogenation treatment without altering significantly the initial catalyst structures;
- *In situ* regenerability was demonstrated by successfully running four consecutive 60 h runs with a reductive regeneration performed between two adjacent runs;
- Further research is needed to more fundamentally understand the nature and role of metal dopants and possible existence of other deactivation mechanisms occurring over a longer operation time frame.

Associated Content

Supporting Information

This material is available free of charge via the Internet at http://pubs.acs.org.

Catalyst bed configurations and temperature profiles employed for 2-stage hydroprocessing runs (Fig. S1); XPS analysis results for a passivated Ni-doped Mo_2C (Fig. S2).

Author Information

Corresponding Author

*E-mail: choijs@ornl.gov.

Notes

The authors declare no competing financial interest.

Acknowledgements

This research was supported by the U.S. Department of Energy, Office of Energy Efficiency and Renewable Energy, Bioenergy Technologies Office. A portion of this research was conducted at ORNL's Center for Nanophase Materials Sciences, which is a DOE Office of Science User Facility. We would like to thank our colleagues for their technical assistance and useful discussion particularly Daniel Santosa and Susanne Jones at PNNL and Jong Keum, Will Brookshear, Josh Pihl, John Henry, and Kevin Cooley at ORNL.

References

1 A.V. Bridgwater, *Biomass Bioenergy*, 2012, **38**, 68.

2 A. Oasmaa, D. C. Elliott and S. Müller, *Environ. Prog. Sus. Energy*, 2009, **28**, 404.

3 M. S. Talmadge, R. M. Baldwin, M. J. Biddy, R. L. McCormick, G. T. Beckham, G. A. Ferguson, S. Czernik, K. A. Magrini-Bair, T. D. Foust, P. D. Metelski, C. Hetrick and M. R. Nimlos, *Green Chem.*, 2014, **16**, 407.

4 D. C. Elliott, *Energy Fuels*, 2007, **21**, 1792.

5 A. H. Zacher, M. V. Olarte, D. M. Santosa, D. C. Elliott and S. B. Jones, *Green Chem.*, 2014, **16**, 491.

6 E. Butler, G. Devlin, D. Meier and K. McDonnell, *Renew. Sus. Energy Rev.*, 2011, **15**, 4171.

7 H. Wang, J. Male and Y. Wang, *ACS Catal.*, 2013, **3**, 1047.

8 E. Furimsky, *Catal. Today*, 2013, **217**, 13.

9 H. Wang and Y. Wang, *Top. Catal.*, 2016, **59**, 65.

10 E. Furimsky and F. E. Massoth, *Catal. Today*, 1999, **52**, 381.

11 S. T. Oyama, *Catal. Today*, 1992, **15**, 179.

12 E. Furimsky, *Appl. Catal. A*, 2003, **240**, 1.

13 A.-M. Alexander and J. S. J. Hargreaves, *Chem. Soc. Rev.*, 2010, **39**, 4388.

14 W. Yu, M. Salciccioli, K. Xiong, M. A. Barteau, D. G. Vlachos and J. G. Chen, *ACS Catal.*, 2014, **4**, 1409.

15 K. Xiong, W.-S. Lee, A. Bhan and J. G. Chen, *ChemSusChem*, 2014, **7**, 2146.

16 W.-S. Lee, Z. Wang, R. J. Wu and A. Bhan, *J. Catal.*, 2014, **319**, 44.

17 P. M. Mortensen, H. W. P. de Carvalho, J.-D. Grunwaldt, P. A. Jensen and A. D. Jensen, *J. Catal.*, 2015, **328**, 208.

18 E. Santillan-Jimenez, M. Perdu, R. Pace, T. Morgan and M. Crocker, *Catalysts*, 2015, **5**, 424.

19 J.-S. Choi, V. Schwartz, E. Santillan-Jimenez, M. Crocker, S. A. Lewis Sr., M. J. Lance, H. M. Meyer III and K. L. More, *Catalysts*, 2015, **5**, 406.

20 E. F. Mai, M. A. Machado, T. E. Davies, J. A. Lopez-Sanchez and V. Teixeira da Silva, *Green Chem.*, 2014, **16**, 4092.

21 J. S. Lee, S. T. Oyama and M. Boudart, *J. Catal.*, 1987, **106**, 125.

22 J.-S. Choi, B. L. Armstrong, V. Schwartz, US Pat., 9 012 349, 2015.

23 M. Boudart and G. Djéga-Mariadassou, in *Kinetics of Heterogeneous Catalytic Reactions*, Princeton University Press, Princeton, 1984, pp. 25-26.

24 D. C. Elliott, H. Wang, R. French, S. Deutch and K. Iisa, *Energy Fuels*, 2014, **28**, 5909.

25 R. Kojima and K. Aika, *Appl. Catal. A: Gen.*, 2001, **219**, 141.

26 K. T. Jung, W. B. Kim, C. H. Rhee and J. S. Lee, *Chem. Mater.*, 2004, **16**, 307.

27 J.-S. Choi, G. Bugli and G. Djéga-Mariadassou, *Stud. Surf. Sci. Catal.*, 2000, **130**, 2885.

28 D. C. Elliott and G. G. Neuenschwander, in *Developments in Thermochemical Biomass Conversion*, ed. A. V. Bridgwater and D. G. B. Boocock, Blackie Academics & Professional, London, 1996, Vo. 1, pp. 611-621.

29 F. De Miguel Mercader, P. J. J. Koehorst, H.J. Heeres, S. R. A. Kersten and J. A. Hogendoorn, *AIChE J*, 2011, **57**, 3160.

30 T. G. Kelly and J. G. Chen, *Green Chem.* 2014, **16**, 777.

31 M. S. Talmadge, R. M. Baldwin, M. J. Biddy, R. L. McCormick, G. T. Beckham, G. A. Ferguson, S. Czernik, K. A. Magrini-Bair, T. D. Foust, P. D. Metelski, C. Hetrick and M. R. Nimlos, *Green Chem.*, 2014, **16**, 407.

32 D. R. Stellwagen and J. H. Bitter, *Green Chem.*, 2015, **17**, 582.

33 J. S. Lee, M. H. Yeom, K. Y. Park, I.-S. Nam, J. S. Chung, Y. G. Kim and S. H. Moon, *J. Catal.*, 1991, **128**, 126.

34 J.-S. Choi, G. Bugli and G. Djéga-Mariadassou, *J. Catal.*, 2000, **193**, 238.

35 S. Jones, P. Meyer, L. Snowden-Swan, A. Padmaperuma, E. Tan, A. Dutta, J. Jacobson and K. Cafferty, *Process Design and Economics for the Conversion of Lignocellulosic Biomass to Hydrocarbon Fuels - Fast Pyrolysis and Hydrotreating Bio-Oil Pathway*, Technical Report, PNNL-23053, NREL/TP-5100-61178, 2013.

36 K. Xiong, W. Yu, D. G. Vlachos and J. G. Chen, *ChemCatChem*, 2015, **7**, 1402.

37 P. Da Costa, J.-L. Lemberton, C. Potvin, J.-M. Manoli, G. Perot, M. Breysse, G. Djéga-Mariadassou, Catal. Today 65 (2001) 195-200.

Table 1. Bulk composition of passivated Mo carbide catalysts[a]

Catalyst	C (wt %)	Mo (wt %)	C/Mo (mol/mol)	Na (wt %)	Ca (wt %)	Co (wt %)	Ni (wt %)	Cu (wt %)
Ni-Mo_2C	5.9	82.3	0.57	0.2	-	-	0.2	-
Ni-Mo_2C-H	5.6	83.6	0.53	0.2	-	-	0.8	-
Cu-Mo_2C	5.3	78.9	0.54	0.2	-	-	-	0.1
Co-Mo_2C	5.8	84.0	0.55	0.3	-	0.2	-	-
Ca-Mo_2C	5.2	83.6	0.50	0.2	0.3	-	-	-

[a] C and metal contents determined by combustion and ICP-AES methods, respectively.

Table 2. Morphological and crystallographic properties of passivated Mo carbide catalysts

Catalyst	Surface area (m^2/g)	Pore volume (cc/g)	Pore size (nm)	Particle size (nm)[a]	Crystallite size (nm)[b]
Ni-Mo_2C	9	0.04	18	73	19
Ni-Mo_2C-H	11	0.05	19	60	17
Cu-Mo_2C	23	0.06	9	29	18
Co-Mo_2C	13	0.04	12	51	17
Ca-Mo_2C	2	0.03	49	330	34

[a] Estimated from BET surface area.

[b] Estimated from XRD peak broadening for (101) plane.

Table 3. Surface composition of passivated Mo carbide catalysts[a]

Catalyst	C (wt %)	Mo (wt %)	C/Mo (mol/mol)	Na (wt %)	Ca (wt %)	Co (wt %)	Ni (wt %)	Cu (wt %)	O (wt %)
Ni-Mo_2C	12.2	78.8	1.2	0.1	-	-	0.3	-	8.7
Ni-Mo_2C-H	7.6	80.5	0.8	0.1	-	-	0.4	-	11.5
Cu-Mo_2C	11.4	73.9	1.2	0.0	-	-	-	0.3	14.4
Co-Mo_2C	19.5	72.0	2.2	0.3	-	0.3	-	-	7.9
Ca-Mo_2C	6.4	77.1	0.7	0.5	1.7	-	-	-	14.3

[a] Data obtained by XPS after 30 s Ar ion sputtering.

Table 4. Types of C and Mo species present on the surface region of passivated Mo carbide catalysts[a]

Catalyst	C (C-C) (wt %)	C (C-O) (wt %)	C (C-Mo) (wt %)	Mo (Mo-C) (wt %)	Mo (Mo-O) (wt %)	C (C-Mo)/Mo (Mo-C) (mol/mol)
Ni-Mo_2C	6.8	1.8	3.6	73.0	5.7	0.39
Ni-Mo_2C-H	3.3	1.5	2.8	71.0	9.5	0.32
Cu-Mo_2C	7.3	2.4	1.7	58.6	15.3	0.23
Co-Mo_2C	13.3	3.0	3.2	66.0	6.1	0.38
Ca-Mo_2C	3.2	1.3	1.9	60.0	17.1	0.26

[a] Data obtained by XPS after 30 s Ar ion sputtering.

Table 5. 2-stage hydroprocessing reactor operating conditions

Catalyst code	Baseline	Ni-Mo_2C	Ni-Mo_2C-H	Cu-Mo_2C	Co-Mo_2C	Ca-Mo_2C
Stage 1 catalyst	Sulfided Ru/C	Ni-doped Mo_2C	Ni-doped Mo_2C	Cu-doped Mo_2C	Co-doped Mo_2C	Ca-doped Mo_2C
Stage 2 catalyst	Sulfided $NiMo/Al_2O_3$	Ni-doped Mo_2C	Ni-doped Mo_2C	Cu-doped Mo_2C	Co-doped Mo_2C	Ca-doped Mo_2C
Stage 1 catalyst mass, g	13.8	12.3	35.6	14.8	16.7	16.8
Stage 2 catalyst mass, g	20.0	12.3	35.6	14.8	16.7	16.8
Stage 1 catalyst volume, mL	31	12.5	35	12	15	14
Stage 2 catalyst volume, mL	31	12.5	35	12	15	14
Stage 1 LHSV, h^{-1}	0.17	0.24	0.25	0.30	0.27	0.29
Stage 2 LHSV, h^{-1}	0.17	0.24	0.25	0.30	0.27	0.29
Stage 1 WHSV, h^{-1}	0.44	0.29	0.29	0.29	0.29	0.29
Stage 2 WHSV, h^{-1}	0.31	0.29	0.29	0.29	0.29	0.29
Stage 1 temperature, °C	190	180	180	180	180	180
Stage 2 temperature, °C	400	400	400	400	400	400
Pressure, MPa	12.4	12.1	12.5	12.1	12.1	12.3
H_2/bio-oil, mL/mL	1935	1700	1680	1700	1700	1680

Table 6. Properties of feed bio-oil and hydroprocessed oil products

TOS (h)	C (wt %, dry)	H (wt %, dry)	H/C ratio (dry basis)	O (wt %, dry)	Moisture (wt %)	N (wt %, wet)	S (wt %, wet)	TAN (mg KOH/g)	Density (g/mL)
Feed bio-oil									
	53.3	6.8	1.53	39.9	30.0	<0.05	<0.02	77	1.200
Ni-Mo_2C									
48-54	NM[a]	NM	NM	NM	1.55	NM	NM	<1	0.869
Ni-Mo_2C-H (higher Ni doping level)									
48-54	85.8	12.9	1.79	1.29	<0.5	<0.05	<0.02	<0.01	0.824
49-55 2nd run	85.4	13.0	1.82	1.55	<0.5	<0.05	<0.02	<0.01	0.834
50-54 3rd run	85.7	12.9	1.79	1.45	<0.5	<0.05	<0.02	<0.01	0.828
48-54[b] 4th run	84.6	12.8	1.80	2.49	<0.5	0.07	<0.02	<0.01	0.845
Cu-Mo_2C									
48-54	88.2	12.0	1.63	1.54	0.89	0.10	0	0.07	0.876
Co-Mo_2C									
48-54	87.2	11.1	1.53	3.24	0	0.24	0	0.58	0.893
Ca-Mo_2C									
48-54[c]	76.6	10.2	1.60	13.0	3.35	0.30	0	5.22	0.949
Baseline (RuS_2/C + $NiMoS/Al_2O_3$)									
43-55	86.3	13.0	1.79	0.65	<0.5	<0.05	<0.02	<0.01	0.835

[a] Not measured.

[b] WHSV = 0.436 h^{-1}.

[c] Stage 2 temperature = 420 °C.

Table 7. ICP-AES analysis for a Ni-doped Mo carbide (Ni-Mo_2C-H) before and after 240 h hydroprocessing testing (ppm)

	Fresh	Tested Stage 1, Upper	Tested Stage 1, Lower	Tested Stage 2
A1	108	562	294	209
Ca	56	2425	328	5019
Cr	< 45	118	392	505
Fe	< 45	433	914	3652
K	119	122	116	237
Mg	< 45	61	185	1792
Mn	< 45	67	65	844
Na	526	132	121	119
Ni	7821	6986	8400	5938
P	< 45	487	313	< 45
Si	< 45	77	47	40
S	< 45	2789	3772	3619
Zr	64	79	96	70

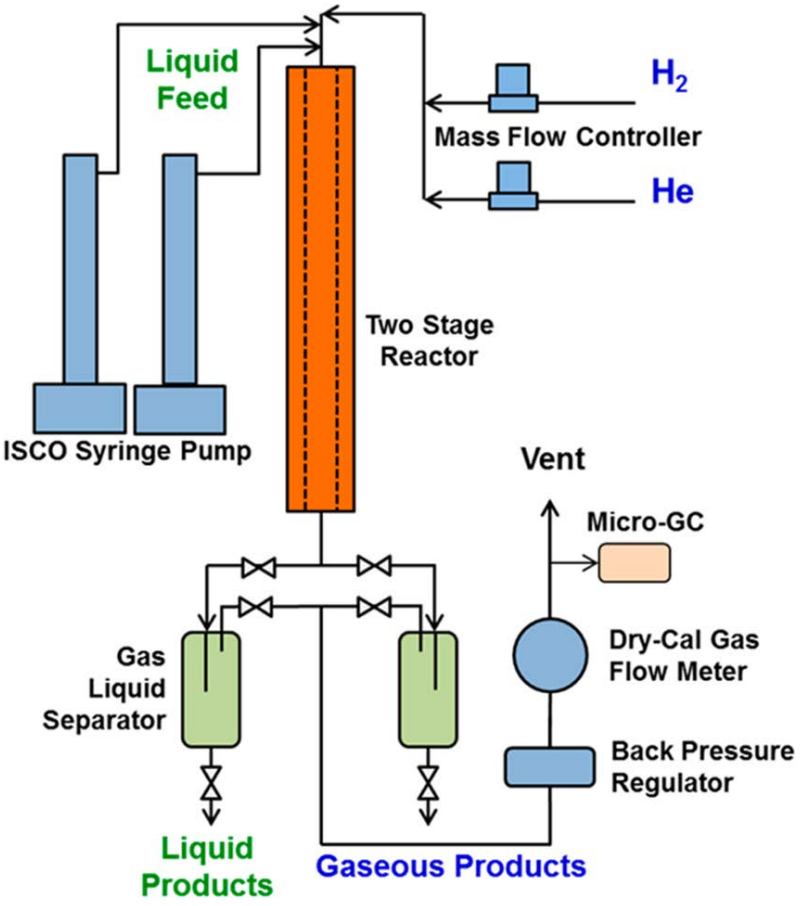

Fig. 1 Schematic of the fixed bed reactor used for the hydroprocessing experiments.

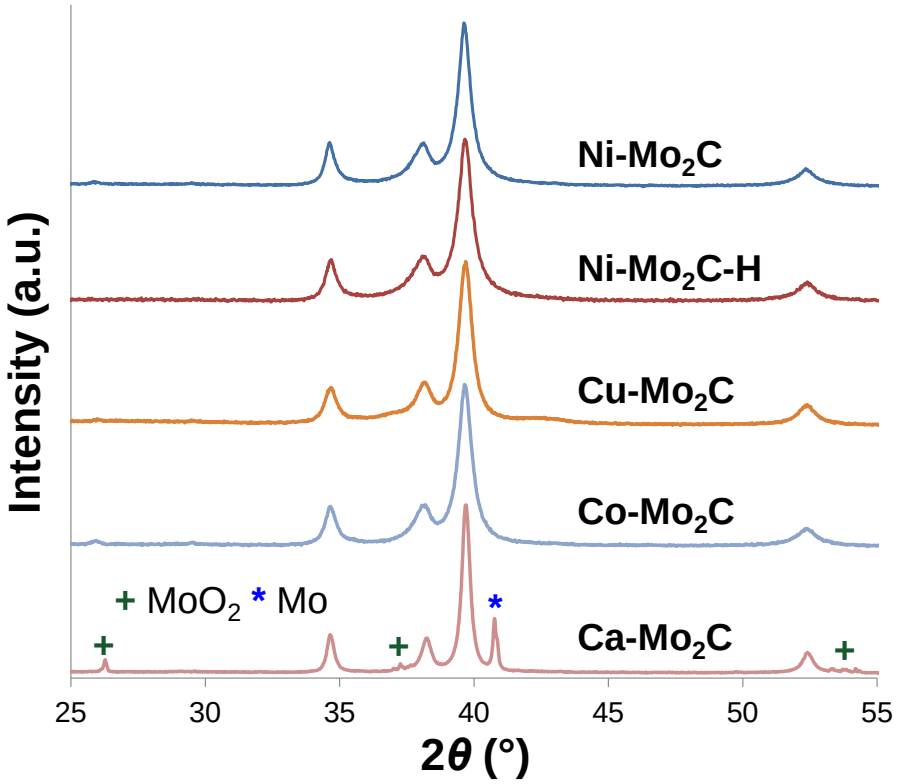

Fig. 2 XRD patterns of fresh Mo_2C catalysts.

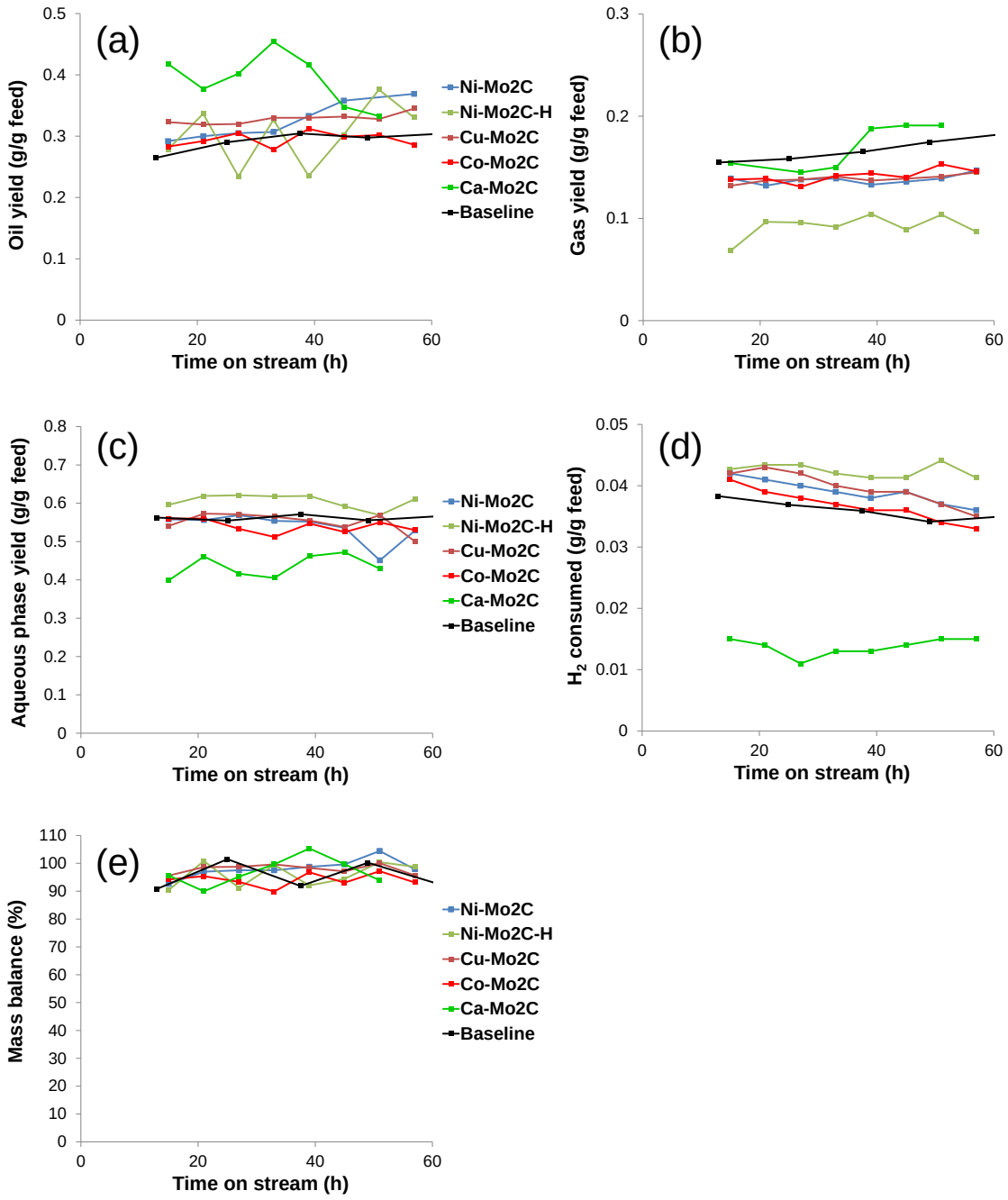

Fig. 3 Bio-oil hydroprocessing results as a function of time on stream: (a) oil yield, (b) gas yield, (c) aqueous phase yield, (d) H_2 consumption, and (e) overall mass balance. For the Ca-Mo_2C catalyst run, the stage 2 temperature was higher at 420 °C from 36 to 54 h TOS; the run was terminated at TOS=54 h due to over 100 psi pressure drop buildup across the bed.

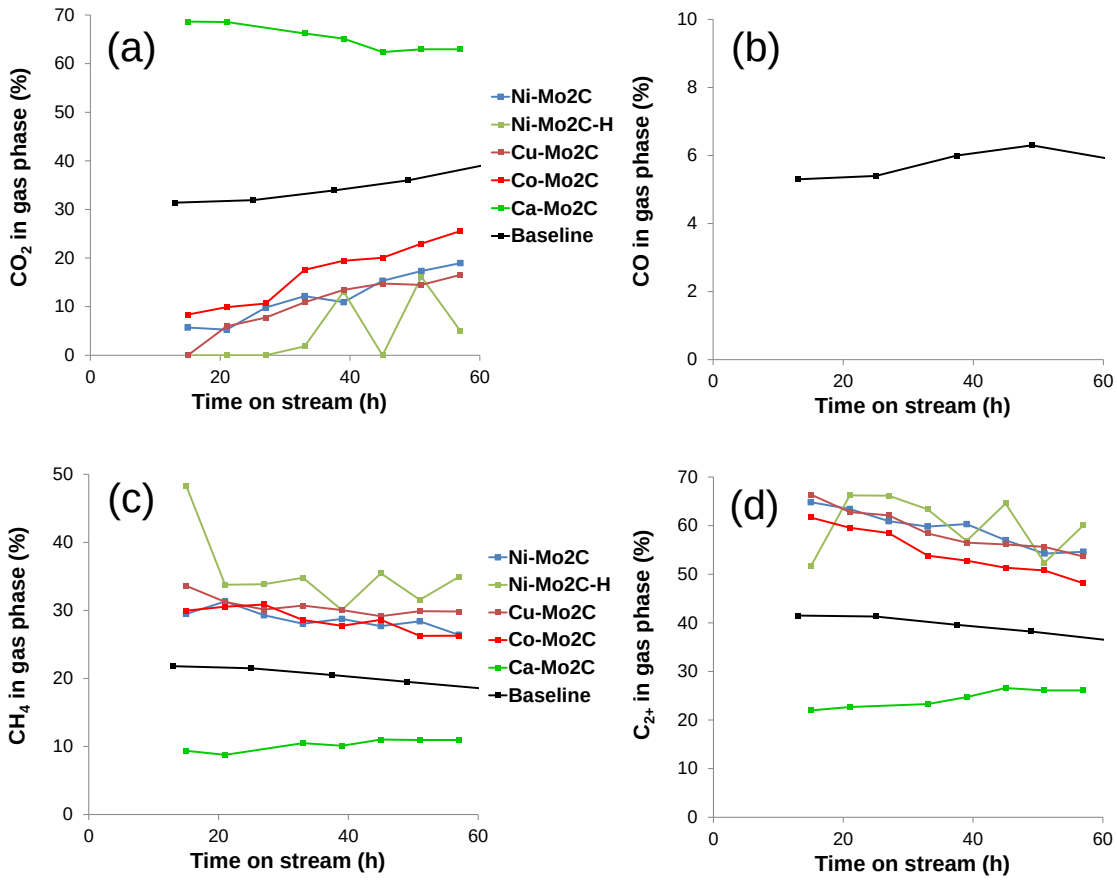

Fig. 4 Composition of gas produced during bio-oil hydroprocessing (volume percent, H_2-free basis): (a) CO_2, (b) CO, (c) CH_4, and (d) C_{2+} hydrocarbons: C_2H_6 + C_3H_8 + C_4H_{10} +C_5H_{12}. For the Ca-Mo_2C catalyst run, the stage 2 temperature was higher at 420 °C from 36 to 54 h TOS; the run was terminated at TOS=54 h due to over 100 psi pressure drop buildup across the bed.

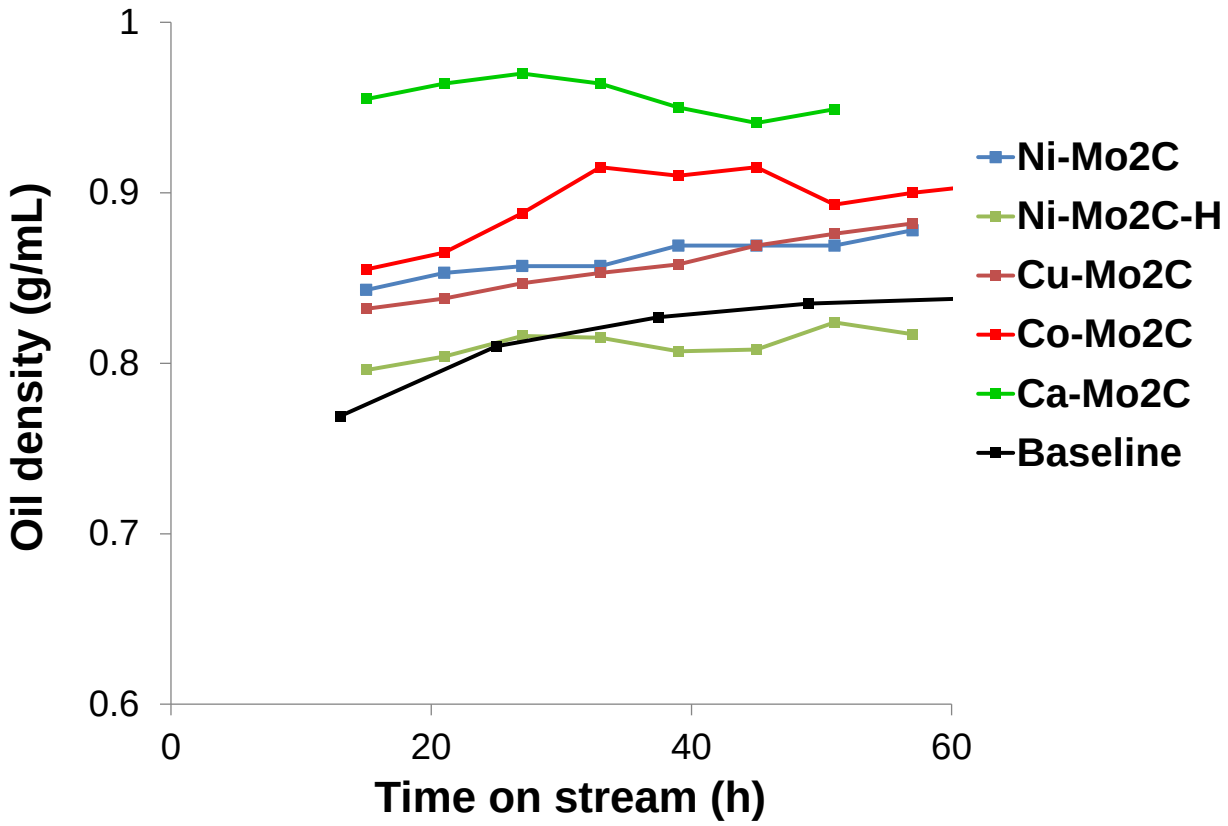

Fig. 5 Density of hydroprocessed bio-oil as a function of time on stream. For the Ca-Mo_2C catalyst run, the stage 2 temperature was higher at 420 °C from 36 to 54 h TOS; the run was terminated at TOS=54 h due to over 100 psi pressure drop buildup across the bed.

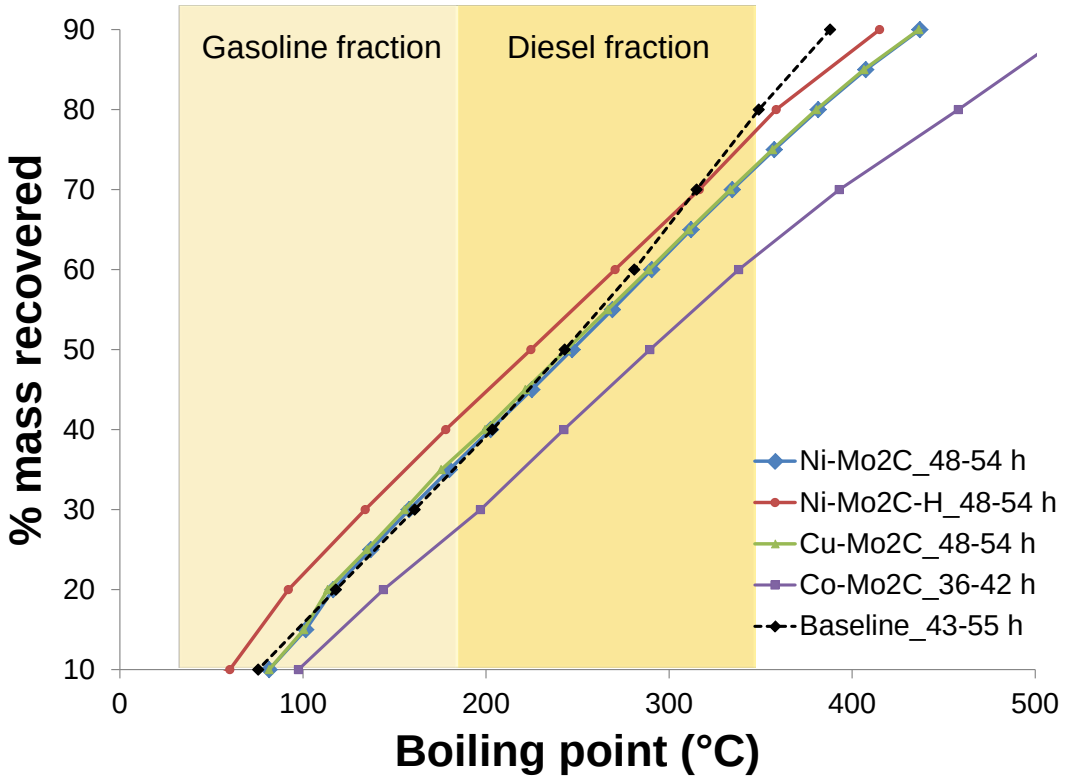

Fig. 6 Simulated distillation analysis of hydroprocessed bio-oils.

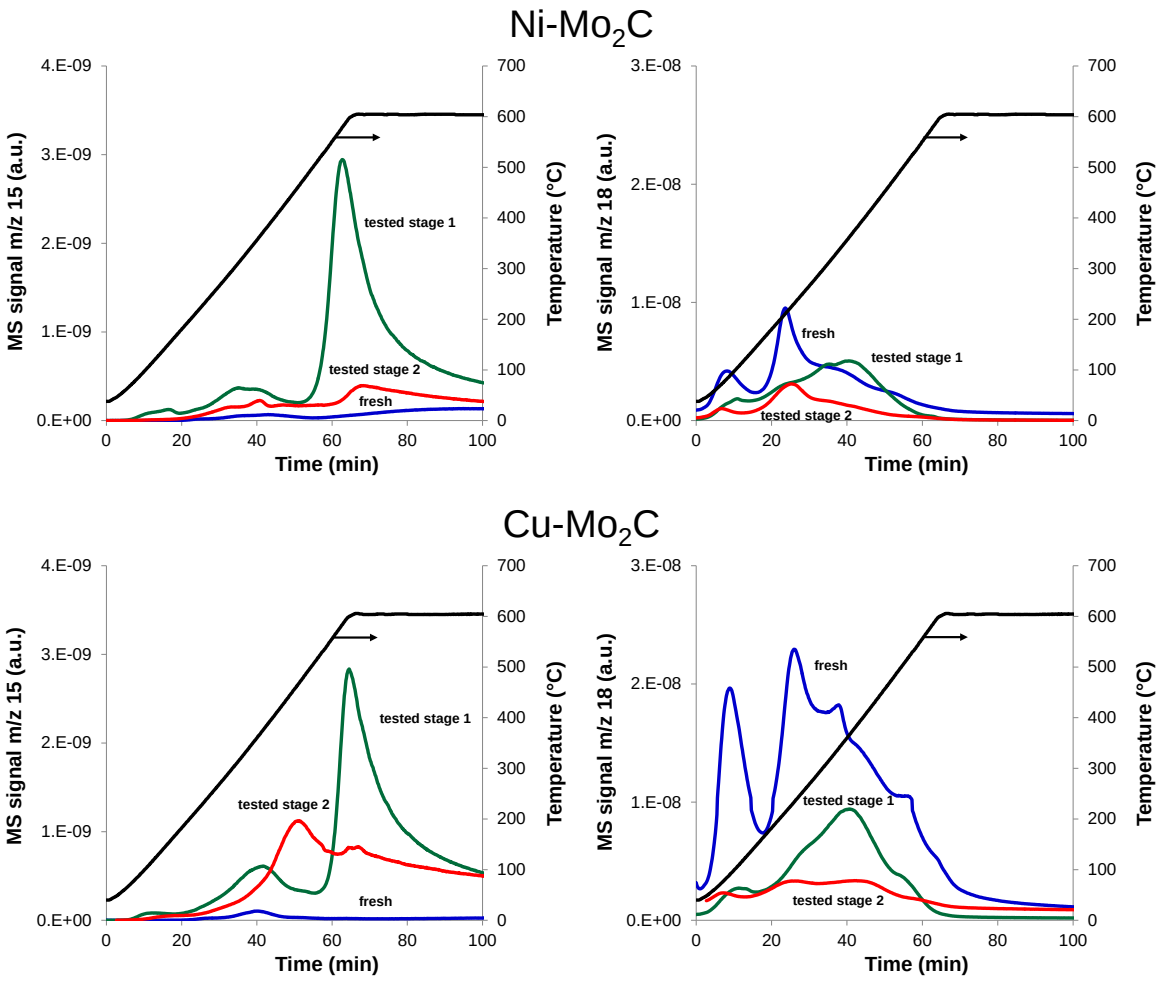

Fig. 7 Temperature-programmed reduction profiles of Mo carbides before (denoted by "fresh") and after a 60 h hydroprocessing runs (denoted by "tested stage 1" and "tested stage 2"). Mass spectrometer m/z 15 and 18 signals correspond to CH_4 and H_2O concentrations, respectively.

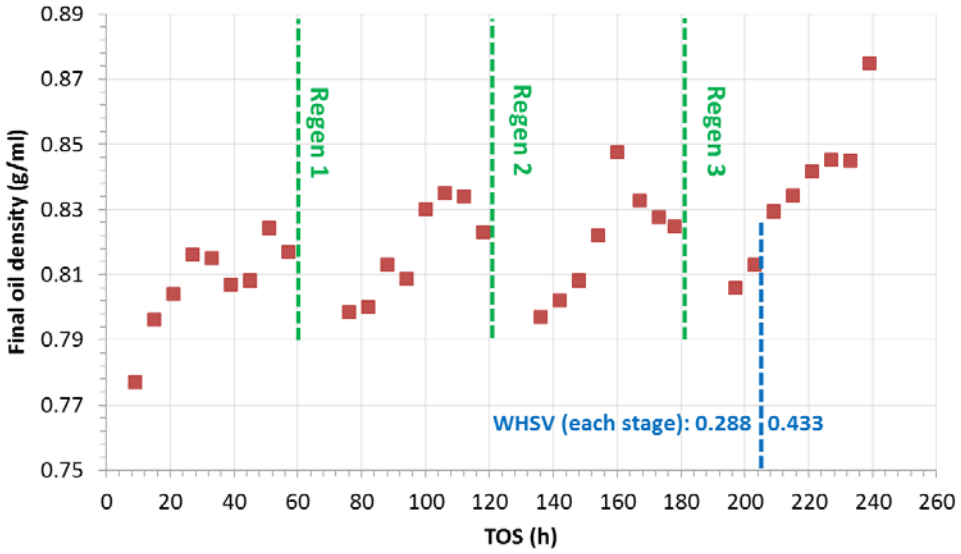

Fig. 8 Density of hydroprocessed bio-oil as a function of time on stream during performance evaluation of the Ni-Mo_2C-H catalyst. Four consecutive 60 h runs were performed with a reductive decoking step between two adjacent runs.

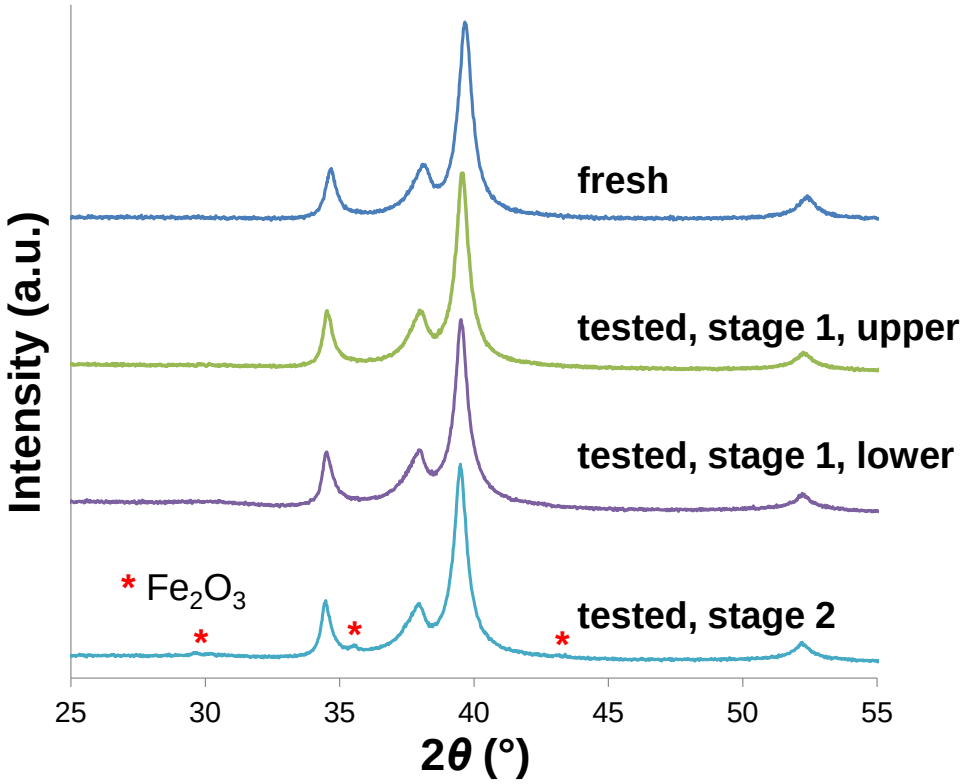

Fig. 9 XRD patterns of Ni-Mo_2C-H catalyst before and after 240 h hydroprocessing.

Table of Contents Graphic

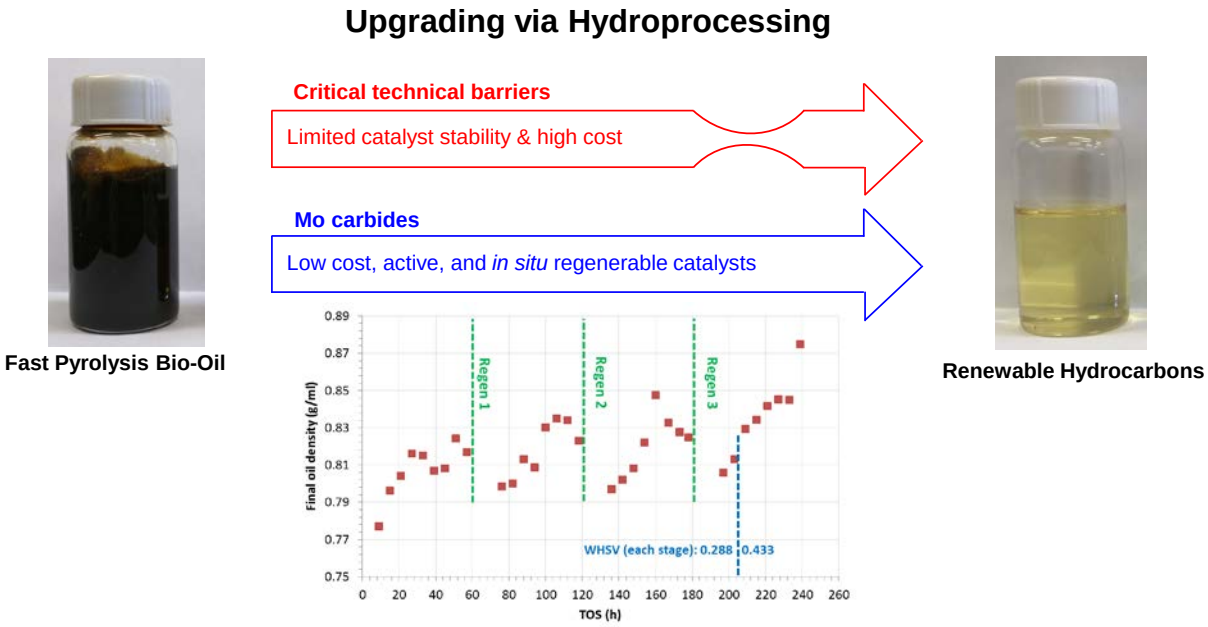

Synopsis

Mo carbides possess promising properties as fast pyrolysis bio-oil hydroprocessing catalysts including low cost, activity, durability, and *in situ* regenerability.